Published in final edited form as:
Biochemistry. 2011 June 21; 50(24): 5426–5435. doi:10.1021/bi200377c.

HD Exchange and PLIMSTEX Determine the Affinities and Order of Binding of Ca^{2+} with Troponin C

Richard Y-C. Huang, **Don L. Rempel**, and **Michael L. Gross***
Department of Chemistry, Washington University in St. Louis, St. Louis, MO 63130

Abstract

Troponin C (TnC), present in all striated muscle, is the Ca^{2+}-activated trigger that initiates myocyte contraction. The binding of Ca^{2+} to TnC initiates a cascade of conformational changes involving the constituent proteins of the thin filament. The functional properties of TnC and its ability to bind Ca^{2+} have significant regulatory influence on the contractile reaction of muscle. Changes in TnC may also correlate with cardiac and various other muscle-related diseases. We report here the implementation of the PLIMSTEX strategy (Protein Ligand Interaction by Mass Spectrometry, Titration and H/D Exchange) to elucidate the binding affinity of TnC with Ca^{2+} and, more importantly, to determine the order of Ca^{2+} binding of the four EF hands of the protein. The four equilibrium constants, $K_1 = (5 \pm 5) \times 10\ M^{-1}$, $K_2 = (1.8 \pm 0.8) \times 10^7\ M^{-1}$, $K_3 = (4.2 \pm 0.9) \times 10^6\ M^{-1}$, and $K_4 = (1.6 \pm 0.6) \times 10^6\ M^{-1}$, agree well with determinations by other methods and serve to increase our confidence in the PLIMSTEX approach. We determined the order of binding to the four EF hands to be III, IV, II, and I by extracting from the H/DX results the deuterium patterns for each EF hand for each state of the protein (apo through fully Ca^{2+} bound). This approach, demonstrated for the first time, may be general for determining binding orders of metal ions and other ligands to proteins.

The basis of muscle contraction has been well studied over four decades. There are primarily two types of proteins involved in this process: troponin and tropomyosin (*1-11*). Muscle contraction is initiated by an increase in intracellular free Ca^{2+} concentration and is controlled by the binding of Ca^{2+} to troponin (*1-3, 8-10, 12-17*). Troponin, which is present in skeletal and cardiac muscle of various species of mammals, birds, and some invertebrates, has three subunits: troponin C (TnC), troponin T (TnT), and troponin I (TnI). Each subunit plays a special rule in modulating the movement of muscle filament.

Troponin C, which is the subject of this study, is an 18 kDa protein that is structurally homologous in skeletal and cardiac muscle (*1, 3*) but has different Ca^{2+} stoichiometry in these two tissues. Skeletal troponin C has four helix-loop-helix motifs (EF hands) that bind to Ca^{2+}. The EF-hand motif, which is a conserved structure first identified in parvalbumins (*18*), allows Ca^{2+} to interact with carboxyl and hydroxyl groups of amino-acid sidechains located at positions 1, 3, 5, 7, 9, and 12 of a 12-membered loop (*1, 19*). One of the EF hands (EF-I) in cardiac troponin C is defunct so the protein binds only three Ca^{2+} (*1, 2, 7, 20-23*). In skeletal troponin C, two of four EF hands are located in the C-terminal (EF-III and EF-IV) and have higher affinities for Ca^{2+} ($K_a \sim 10^7\ M^{-1}$) than the other two EF hands; they are usually saturated with Ca^{2+} or Mg^{2+} in tissue. The binding of Ca^{2+} at these two sites helps

* To whom correspondence should be addressed: Department of Chemistry, Washington University in St. Louis, Campus Box 1134, St. Louis, MO 63130. Telephone: (314) 935-4814, Fax: (314) 935-7484, mgross@wustl.edu.

SUPPORTING INFORMATION AVAILABLE

Supplemental figures are included in the Supporting Information section. This material is available free of charge via the Internet at http://pubs.acs.org.

maintain the interaction between the C-terminus of troponin C, the N-terminus of troponin I, and the C-terminus of troponin T (*1*, *24-27*). The latter subunit binds to tropomyosin on the muscle thin filament, serving as a key in complex formation. When the two N-terminal EF hands (EF-I and EF-II), which have lower affinities for Ca^{2+} ($K_a \sim 10^5$-10^6 M^{-1}), bind to Ca^{2+}, troponin C undergoes a conformational change to form a hydrophobic core (*15*, *23*, *26*, *28-30*). The inhibitor region on the C-terminus of troponin I then interacts with this core and releases tropomyosin and actin. The free actins are able to interact with the myosin heads on the thick filament and produce muscle contraction (*1-3*).

The Ca^{2+} binding to troponin C and its relation to muscle-contraction disorders have implications in cardiac-related diseases. The amino-acid sequence of troponin C and the phosphorylation of troponin I induced by over-activation of protein kinase A and C (*31*, *32*) affect the binding of Ca^{2+} to troponin C. Newly designed drugs interact with troponin C and adjust its affinities to Ca^{2+} (*33*, *34*).

The Ca^{2+}-binding and protein-target binding properties of troponin C have been the subjects of numerous studies using NMR (*21*, *25*, *35-37*), calorimetry (*38*) and fluorescence (*26*). Hydrogen/deuterium exchange (H/DX) coupled with mass spectrometry is another powerful method to study protein conformation, protein-protein or protein-ligand interactions (*39-46*). With H/DX, one can measure the relative rates of exchange of backbone amide hydrogen with deuterium and thereby follow changes in H-bonding, which often is parallel to relative solvent accessibilities. Recently, H/DX was applied to study the regulatory function of human cardiac troponin complex and the conformational changes of troponin complex induced by Ca^2 binding (*47*, *48*).

We describe here the use of PLIMSTEX (Protein–ligand interactions by mass spectrometry, titration, and H/D exchange) (*49-51*) to determine again the affinities of Ca^{2+} to rabbit skeletal troponin C. The purpose of the determination is to test the ability of PLIMSTEX to extract these values in a complex 4:1 interaction. From the determined affinities (equilibrium constants), we calculated the fractional species for the variousTnC-Ca^2 states as a function of [Ca^{2+}]. The deuterium exchange patterns of four peptic peptides representing the four EF hands of rabbit skeletal troponin C (EF-I peptide 28-44: DADGGGDISVKELGTVM; EF-II peptide 63-73: EVDEDGSGTID; EF-III peptide 100-109: FRIFDRNADG; EF-IV peptide 136-149: MKDGDKNNDGRIDF) were then measured. Guided by the fractional species calculation, the deuterium patterns for each EF-hand were measured as a function of the various Ca^{2+} binding states (i.e., 0, 1, 2, 3, and 4) to determine how D distributions change as a function of the binding states. Previous efforts to elucidate the binding properties of Ca^{2+} to troponin C used NMR, fluorescence measurement, Ca^{2+} ion-selective electrode measurements, and mutagenesis (*36*, *37*, *52*, *53*). Although some insights were achieved, a full understanding on the Ca^{2+} binding order is still lacking. Our strategy provided data that, for the first time, gives the binding order of Ca^{2+} to full length troponin C in a single and relatively simple experiment. Our ultimate goal is to extend the approach to study the effect of troponin I and troponin T on the affinities and orders of binding of Ca^{2+} to troponin C.

EXPERIMENTAL PROCEDURE

a. Materials

Rabbit skeletal Troponin C (TnC) was purchased from Ocean Biologics Inc (Seattle, WA). Potassium chloride, calcium chloride, EGTA tetra sodium salt [ethylene-bis(oxyethylenenitrilo)tetraacetic acid tetrasodium], and HEPES hemisodium salt [*N*-(2-hydroxyethyl)piperazine-*N*′-(2-ethanesulfonic acid) hemisodium salt] were purchased from Sigma-Aldrich (St.Louis, MO). Deuterium oxide was purchased from Cambridge Isotope

Laboratories Inc (Andover, MA). Immobilized pepsin on agarose was purchased from Pierce (Rockford, IL).

b. Apo TnC preparation

TnC was dialyzed against EGTA to obtain apo-TnC. A 1 mL protein solution containing 180 μg of TnC was prepared in 10 mM HEPES and 150 mM KCl. The solution was dialyzed by using Slide-A-Lyzer Dialysis Cassettes 7000 MWCO (Pierce, CA). The dialysis membrane was first boiled two times in 10 mM EGTA for 10 min to remove heavy metals from the membrane and then soaked in deionized H_2O for 10 min. The protein solution was then injected into the cassette and dialyzed against 10 mM HEPES, 150 mM KCl and 1 mM EGTA for 2 h. The buffer was exchanged for fresh buffer, and the solution was dialyzed overnight at 4 °C. The protein solution was then dialyzed against 10 mM HEPES, 150 mM KCl for 3 h, fresh buffer was added, and the protein was dialyzed again for 3 h at 4 °C. The concentration of the final protein solution was measured by using a UV spectrophotometer at 280 nm absorption. The protein solution was stored at -80 °C.

c. H/D exchange (H/DX) protocol

H/DX was initiated by diluting the protein solution 1:40 into D_2O buffer (10 mM HEPES, 150 mM KCl) at 25 °C. At various times, H/DX was quenched by adding sufficient 1 M HCl at 0 °C to give a final pH of 2.5.

For Global protein H/DX experiments, a quenched protein solution was loaded onto a C8 guard column (1 mm × 15 mm, Optimize Technologies, Oregon, City, OR). The column was pre-equilibrated with 200 μL 0.2% formic acid in water (0 °C). After loading the protein solution, the column was washed with 250 μL 0.2% formic acid in ice cold normal water (0 °C) to back-exchange the labile sites on side chains. The protein was eluted by using a gradient from 5% to 40% solvent B in 3 min, 40% to 100% solvent B in 3 min and back to 5% solvent B in 2 min. (Waters CapLC, Manchester, U.K; solvent A, water containing 0.1% formic acid; solvent B, acetonitrile containing 0.1% formic acid).

For peptide-level H/DX experiments, 5 μL of immobilized pepsin on agarose was added to the solution. Protein digestion took place at 0 °C for 3 min. The final solution was centrifuged for 2-3 s to bring down the agarose beads. The peptide-containing supernatant was then loaded onto a C18 guard column (1 mm × 15 mm, Optimize Technologies, Oregon, City, OR). The column was pre-equilibrated with 200 μL of 0.2% formic acid in water (0 °C). After loading, the column was washed with 250 μL of aqueous 0.2% formic acid (H_2O) to back-exchange the labile sites. The protein was eluted by using a gradient from 5% to 35% solvent B in 3 min, 35% to 80% solvent B in 4 min, 80% to 100% solvent B in 1 min and back to 5% solvent B in 2 min. All LC connection lines were immersed in a water-ice (0 °C) bath. (Waters nanoACQUITY UPLC, Manchester, U.K; solvent A, water containing 0.1% formic acid; solvent B, acetonitrile containing 0.1% formic acid).

d. LC-ESI/MS analysis with a Q-TOF mass spectrometer

Global protein H/DX results were acquired on a Waters (Micromass) (Manchester, U.K.) Q-TOF Ultima spectrometer equipped with a Z-spray ESI source. The instrument settings were: capillary voltage, 3.0 kV; cone voltage, 80 V; source and desolvation temperatures, 80 °C and 180 °C, respectively. The cone and desolvation gas flow rates were 40 and 400 L/h, respectively. The MS profile used for quadrupole transmission was: scan from *m/z* 500, dwell for 5% of the scan time, ramp to *m/z* 1000 for 45% of the scan time, and then dwell at *m/z* 1000 for 50% of the scan time.

Peptide-level H/DX results were acquired on a Maxis (Bruker) (Bremen, Germany) Q-TOF spectrometer. The instrument settings were: capillary voltage, 3.8 kV; nebulizer gas, 0.4 Bar; drying gas flow rate and temperature, 4.0 L/min and 180 °C; funnel RF, 400 V(pp).

e. LC-ESI/MS/MS analysis of protein digests

To establish the peptide profile from the pepsin digestion of TnC, 100 pmol TnC was digested with pepsin for 3 min, and the peptides were identified by accurate mass and sequencing by product-ion analysis on a Thermo LTQ XL Orbitrap (Thermo Fisher, San Jose, CA). Samples were loaded and eluted by using an Ultra 1D+ UPLC and autosampler (Eksigent, Dublin, CA). A 75 μm diameter column was pulled with a laser-based column puller (Sutter Instruments, Novato, CA) and packed with 12 cm of Magic C18AQ reverse phase media (Michrom Bioresources, Auburn, CA). The column was interfaced via a nanospray source (New Objective, Woburn, MA) and eluted with a 60 min gradient from 2-98% solvent B (acetonitrile with 0.1% formic acid). The spray voltage was 2.0 kV, and the capillary temperature was 200 °C. One full mass spectral acquisition triggered six scans of MS/MS whereby the most abundant precursor ions were activated for sequencing. The product-ion spectra (MS/MS) data were centroided during the acquisition.

f. Mascot database search

Thermo RAW files were processed using extract_msn (2007 version 4.0, Thermo Fisher, San Jose, CA) with a grouping tolerance of 0.8 Da, an intermediate scan setting of 1, and a minimum of 1 scan per group. The NCBI nonredundant database (version 20080718, restricted to mammals) was searched by using MASCOT 2.2.06 (Matrix Science, Oxford, U.K.) with the following settings: enzyme, none; MS tolerance, 10 ppm; MS/MS tolerance, 0.8 Da; maximum number of missed cleavages, 3; peptide charge of 1+, 2+ and 3+; oxidation of methionine was set as variable modification.

g. Data analysis

The uptake of deuterium by the global protein was the average mass differences between the masses of the deuterated protein and the undeuterated protein. The back-exchange rate was measured to be one deuterium loss per minute (*45*). No correction for back exchange was applied because the time between sample quench and the measurement with the mass spectrometer was less than 3 min, and all data were treated consistently. For global protein analysis, deconvoluted spectra were generated by using the MaxEnt1 algorithm (MassLynX version 4.0). The parameter settings were: resolution, 1.00 Da/channel; uniform Gaussian width at half height, 1.00 Da; minimum intensity ratios, 33% for left peaks and right peaks.

h. Kinetic modeling

The global protein kinetic data were fit with a fixed-rate-constant binning model by MathCAD (Math-Soft. Inc. Cambridge, MA) in which the root mean square (RMS) was minimized (*50*, *51*). All exchangeable H's were separated into four fixed rate-constant bins (k = 10, 1, 0.1, 0.01 min^{-1}). These rate constants were selected because the rates of exchange change measurably in the time frame 0.17 min to 540 min, and the H/DX became relatively constant after 60 min; hence the brackets of 10 min^{-1} (fast exchangers, half-life ~0.07 min) and 0.01 min^{-1} (slow exchangers, half-life ~69 min) were chosen. Although the largest rate constant for H/DX is >100 min^{-1} for unstructured peptides (*54*), we are yet unable to obtain data at the short times that correspond to this rate constant. Three trials were fit separately, and the results were averaged and reported with standard deviations.

i. Titration and species fraction calculation

The method for fitting the titration curve was described previously (*51*). Briefly, there are nine parameters involved in the 1:4 protein-ligand binding systems: K_{a1}, K_{a2}, K_{a3}, K_{a4}, D_0, ΔD_1, ΔD_2, ΔD_3, ΔD_4; K_a is the binding constant; D_0 is the deuterium uptake of protein in the absence of ligands (Apo form); ΔD_x is the difference between the average of deuterium uptake of the complex in the presence of x ligands and that of the apo form. The non-linear least squares fitting utilized the "Minimize" function of MathCAD (Math-Soft. Inc. Cambridge, MA) to minimize the root mean square (RMS) of all inputs by optimizing the parameters being searched. To obtain the nine parameters in single fitting cycle with acceptable precision, a significant number of titration points would be needed (>500) by applying a resampling statistical method (*51*). Because it was difficult to fit the titration curve by varying all nine parameters in one fitting cycle, a repeat fitting cycle strategy was used to obtain the *K*'s and ΔD's values reported here.

The fitting process was started by making a guess of the D's (D_0, ΔD_1, ΔD_2, ΔD_3, ΔD_4) values. The initial values for D_0 was set as experimental data, and the values for ΔD_1, ΔD_2, ΔD_3, ΔD_4 were obtained through a PLIMSTEX experiment at high protein concentration (100 times the $1/K_a$ or K_d as reported previously) (**Supplemental Figure 1**). We fixed these D's values and searched for *K*'s in the initial fitting process. After the four *K*'s (K_{a1}, K_{a2}, K_{a3}, K_{a4}) were obtained, the repeat-fitting processes were then started. In first half cycle, we fixed the *K*'s obtained in the initial process and searched for the *D*'s. We then fixed the ΔD_1, ΔD_2, ΔD_3, and searched for K_{a1}, K_{a2}, K_{a3}, K_{a4}, D_0, and ΔD_4 to finish the cycle. This fitting cycle was repeated until the relative differences between K's values before and after each cycle of fitting were less than 10%. Three trials of experiments were applied with this strategy separately, and the results were averaged and reported with standard deviations.

Once the binding affinities of Ca^{2+} were determined, the information for fractionally bound TnC species as a function of Ca^{2+} was obtained and presented as a deuterium pattern (d_0, d_1, . . .) in which other isotopes (e.g.,^{13}C, ^{15}N, ^{18}O) had been removed by using an isotopic pattern calculation. To obtain these patterns, each mass list from three experimental trials was extracted from their individual spectra as an x,y file (x: mass-to-charge ratio; y: intensity). A program in MathCAD was applied to find the isotopic peak envelope among the list by providing the chemical formula and charge state of the target peptide. The peak area in each envelope was applied for fractional species calculation, and the isotopes (^{13}C, ^{15}N, ^{18}O) were removed from the output by using the information provided via the Isotope Simulation function in Qual Browser 2.0.7 (Xcalibur, Thermo Fisher, San Jose, CA).

RESULTS

a. H/DX kinetics of apo- and holo-TnC

Binding of four Ca^{2+} induces a conformational change in troponin C. Previous studies showed that the structure of the holo (Ca^{2+} saturated) state of skeletal troponin C is more structurally open than the semi-apo state (two Ca^{2+} bound). The center partial-loop structure between the N and C-terminal EF hands forms a less flexible helix whereas the Ca^{2+} is bound to the two EF hands near the N-terminus (EF-I and EF-II) (*1*, *4*, *12*, *55*). A detailed structure of apo-troponin C has eluded determination owing to the unstructured C-terminus in the absence of Ca^{2+} (*37*, *56*).

We began our study by measuring the kinetics of H/DX of rabbit skeletal troponin C in the Ca^{2+} saturated (holo) and Ca^{2+} absent (apo) states (**Figure 1**); the output is a plot of deuterium uptake as a function of exchange times (10 s to 9 h). To generate the holo state of troponin C, we made the protein stock solution (40 μM) containing 10 mM HEPES, 150

mM KCl, and 1 mM $CaCl_2$, pH 7.4. Using KCl mimics physiological conditions, and excess Ca^{2+} (the ratio of Ca^{2+} concentration to protein concentration was 25) insures that the four EF hands of troponin C are saturated with Ca^{2+}. To generate the apo state of troponin C, we replaced $CaCl_2$ with 3 mM EGTA to insure that no Ca^{2+} was present in the protein.

Rabbit skeletal troponin C has 158 exchangeable amide protons (excluding one proline). Because the percentage of D_2O in the experiment was 97%, the maximum number of observable exchange events is 153. After 20 min of H/DX, the mass of apo troponin C shifted by 116 ± 1 Da, indicating that ~75% of the amide sites are exchangeable at this time. This high level of exchange is in accord with the general view that troponin C in solution is highly flexible, dynamic, and solvent-exposed in the absence of Ca^{2+}. In the presence of Ca^{2+}, the number of amides undergoing H/DX decreased to 83 ± 1 Da after 20 min of exchange, indicating that ~32 amide sites no longer exchange as a consequence of Ca^{2+} binding. A more stabilized secondary structure, an increase in hydrogen bonding, a decrease in solvent accessibility of some amide sites, and/or a combination of these factors decreased the H/DX rates.

To understand quantitatively how Ca^{2+} binding affects the exchange rate, we fit the kinetic curve with four exchange rate bins (k = 10, 1, 0.1, 0.01 min^{-1}) (**Table 1**). The results show that the apo state has 79 ± 1 sites with an exchange rate constant of 10 min^{-1}, whereas the holo state has only 26 ± 2 sites with the same rate constant, indicating that ~53 fast-exchanging sites are affected by Ca^{2+} binding. In the holo state, these sites shift to the lower exchange rates including those with an exchange rate constant of 1 min^{-1} where the apo state has 1 ± 1 sites whereas the holo state has 24 ± 2 sites. There are also significant differences for those amides undergoing exchange with a rate constant of 0.01 min^{-1}; whereas the holo state has 61 ± 3 sites, 37 ± 4 amides in the apo state exchange at this corresponding low rate. The overall shift to states having low exchange rate constants is consistent with troponin C possessing a more rigid secondary structure upon Ca^{2+} binding.

b. Affinities for Ca^{2+} binding of troponin C

Several methods can be used to measure the binding affinities for protein-protein interactions and protein-small molecule interactions; these methods include FRET (fluorescence resonance energy transfer) (*57*), NMR (*58*), CD (circular dichorism) (*59*), calorimetry (*60*) and SPR (surface plasmon resonance) (*61*, *62*). Because there is a significant difference in deuterium uptake between apo-TnC and holo-TnC, we can apply PLIMSTEX (Protein–ligand interactions by mass spectrometry, titration, and H/DX) to measure the equilibrium constants for Ca^{2+} binding to TnC (*45*, *4951*, *63*) in a relatively simple experiment.

Our titration format varies the relative concentration of Ca^{2+} and monitors by MS the extent of H/DX as a function of time. Because EF-III and EF-IV are known from previous studies to be high-affinity sites, they are often saturated with Ca^{2+}. To insure the protein was in the full apo state (no bound Ca^{2+}), we carried out a two-step dialysis procedure (see Experimental). The deuterium uptake of the dialyzed TnC was comparable to that of TnC in the presence of EGTA (data not shown), indicating the dialysis was successful in removing Ca^{2+} from the protein. This purified protein sample was used as the starting material for the titration (**Figure 2**); the troponin C concentration for the titration was 0.3 μM, which falls into the range of K_d's determined previously (*64*). The time for H/DX (97% D_2O buffer, 10 mM HEPES, 150 mM KCl, pH 7.4) was necessarily constant at 1 h, a time for which H/DX had become relatively constant, and for which small errors in sampling time would have minimal impact on the titration. We also performed the titration at high protein concentration, 15 μM, which is ~100 times the K_d values (**Supplemental figure 1**). A titration at this protein concentration will usually give a “sharp break” curve that reveals the

stoichiometry of the ligand binding (*49*); in this case, rabbit skeletal troponin C binds four Ca^{2+}, in agreement with previous findings. The other purpose for conducting this "sharp break" titration is to obtain an estimate of the *ΔD*'s values to aid the PLIMSTEX curve fitting process (see Experimental). At high protein concentration, the equilibrium shifts toward the protein-ligand complex, and the resulting *ΔD*'s values will be similar to the actual *ΔD*'s, which report the change in the protein secondary structure owing to each ligand binding.

In this manner, we obtained ΔD_1, ΔD_2, ΔD_3, and ΔD_4 as 6, 15, 31, and 37, respectively. These values serve as the initial guesses for the repeat-fitting cycle described in the experimental section. The relative variations of K_2, K_3 and K_4 all decreased to ~10% after we performed three cycles of the fitting (**Supplemental Figure 2**). Although the relative variation of K_1 was not constrained over each fitting cycle, probably because the number of experimental points is insufficient, its value still is in a reasonable range. Given that the affinities are known and that the main purpose of the study is to investigate the order of binding, we did not pursue the titration further because additional improvements would not affect significantly the determination of the binding order.

Previous studies show that skeletal troponin C has two Ca^{2+} binding sites, EF-III and EF-IV, located near the C-terminus; their binding affinities are comparable at $(2.1 \pm 0.7) \times 10^7$ M^{-1} (*64*). Two additional sites are located near the N-terminus of skeletal troponin C, EF-I and EF-II, and their binding affinities for Ca^{2+} are in the range of 3×10^5 to 5×10^6 M^{-1} (*20*, *64*). Although the equilibrium constants show variability from study to study (possibly because the affinities are relatively small), the consensus is that the equilibrium constants for the N-terminal EF hands are in the range of 10^5-10^6 M^{-1} and smaller than those for the C terminus (*37*).

We fit the titration curve to a non-linear least squares model that was previously described (*51*). The output of the fitting produced four K_a's (**Table 2**), two with high values of $(5 \pm 5) \times 10^7$ M^{-1} and $(1.8 \pm 0.8) \times 10^7$ M^{-1}, which are within a factor of 3 of previous results. The other two K_a's have smaller values of $(4.2 \pm 0.9) \times 10^6$ M^{-1} and $(1.6 \pm 0.6) \times 10^6$ M^{-1}, which are also within the range of values from previous studies. The fitting parameter D_0 (126.5 ± 0.1), which represents the deuterium uptake in the apo state is in agreement with the experimental results (127 ± 2).

c. Fractional species and binding order

The titration study provides us the four equilibrium constants (K_a) for Ca^{2+} binding to troponin C. These values are not new, and they can be determined by other approaches. Remarkable, however, is that three of the four values (K_2, K_3 and K_4) can be extracted with reasonable precision from a single titration, probably because each addition of Ca^{2+} to the protein induces a change in conformation that responds to H/DX. Because the binding affinities are different, it is likely that that Ca^{2+} binding is cooperative and occurs, at least in part, in a stepwise manner.

The next level of information is the order of binding, which we sought to determine by following the H/DX extent at the EF-hand level. One prospect is to examine the deuterium distribution for the various EF hands as a function of Ca^{2+} concentration. These EF-hand regions may be removed from the protein following H/DX as peptides by pepsin digestion and submitted to LC-MS analysis. When an EF hand binds Ca^{2+}, we expect the extent of H/DX will decrease. By identifying the state of Ca^{2+} binding (e.g., 0, 1, 2, 3, 4) for which the change occurs, we should be able to determine in a straightforward way the order for Ca^{2+} binding. The interaction between Ca^{2+} and troponin C at any titration point, however, results in a mixture of Ca^{2+}-binding states, and the deuterium distribution of any given EF hand at

each titration point is of a mixture of different Ca^{2+} bound states. The challenge is to extract from this mixture of states the deuterium distribution of an EF hand for a single state (**Figure 3**).

The four equilibrium constants, determined by PLIMSTEX or any other method, are a source of fractional species information that allow the determination of the population of the various Ca^{2+} states as a function of $[Ca^{2+}]$. We hypothesize that knowing these fractional species will lead us to the required deuterium distributions. To test this hypothesis, we used the previously reported and likely more reliable K_1 value (2.1×10^7 M^{-1}) and the K_2, K_3, and K_4 values (1.8×10^7 M^{-1}, 4.2×10^6 M^{-1}, 1.6×10^6 M^{-1}, respectively) determined by PLIMSTEX to calculate the fractional species as a function of total $[Ca^{2+}]$ and determine the population of the five troponin C species, TnC:xCa^{2+} (x = 0-4) when the protein concentration was 4.2 μM (**Figure 3**). The reason for choosing a literature K_1 is the precision for our K_1 value is not high because the titration is underdetermined, and we don't want that to affect the precision for the fractional species determination. We chose seven Ca^{2+} concentrations from the fractional-species plot, including $[Ca^{2+}]$ = 0 (100% apo TnC) and Ca^{2+} = 2 mM (100% holo TnC) (**Table 3**) for our search for the required deuterium distributions. To obtain the needed experimental data, we conducted H/DX for 1 h in 90% D_2O buffer (10 mM HEPES, 150 mM KCl, pH 7.4), quenched the exchanging solution, digested the protein with pepsin for 3 min on ice-water, and analyzed the peptide mixture by LC/MS.

MS analysis directly gave us the complete isotopic distribution for specific deuterated peptides, but this distribution represents various states of the protein, not the single state we seek. Nevertheless, from these distributions, we can calculate the representative isotopic distribution for each Ca^{2+}-bound troponin C species (see Figure 4 for an example of this idea). The upper left spectrum shows the deuterium-containing isotopic distribution when $[Ca^{2+}]$ = 16.7 μM for the triply charged peptic peptide FRIFDRNADG, which is from the EF-III region. From Table 3, we know that there is 30% TnC-3Ca^{2+} species and 70% of TnC-4Ca^{2+} species in the solution when the total $[Ca^{2+}]$ is 16.7 μM. Because we know the deuterium distribution of this peptide when $[Ca^{2+}]$ = 2 mM (representing 100% TnC-4Ca^{2+} species, lower left in **Figure 4**), we can remove that pattern from the experimental distribution to give the deuterium distribution for the peptide representing this region of the protein when it exists as TnC-3Ca^{2+} (right pattern in **Figure 4**).

To sort out the required isotopic distributions, we implemented an algorithm with Mathcad 2001 Professional (Math-Soft, Inc., Cambridge, MA). We extracted mass lists containing all peptide information from each spectrum and input them into MathCAD as x,y files for peak-finding and fractional-species calculation. The basis for this algorithm is in matrix algebra as given in equation 1.

$$\underset{\text{Matrix A}}{\begin{bmatrix} I_{00} & I_{01} \cdots I_{0m} \\ I_{10} & I_{11} \cdots I_{1m} \\ \vdots & \vdots \\ I_{n0} & I_{n1} \cdots I_{nm} \end{bmatrix}} = \underset{\text{Matrix B}}{\begin{bmatrix} IS_{00} & IS_{01} \cdots IS_{0x} \\ IS_{10} & IS_{11} \cdots IS_{1x} \\ \vdots & \vdots \\ IS_{n0} & IS_{n1} \cdots IS_{nx} \end{bmatrix}} \times \underset{\text{Matrix C}}{\begin{bmatrix} PS_{00} & PS_{01} \cdots PS_{0m} \\ PS_{10} & PS_{11} \cdots PS_{1m} \\ \vdots & \vdots \\ PS_{x0} & PS_{x1} \cdots PS_{xm} \end{bmatrix}} \quad (1)$$

In this equation, matrix A is the input of the experimental results; that is, the isotopic abundances for a single peptide I, from peak 0 to peak n as a function of the various ligand concentrations. Matrix C provides the fractional species information; that is, the population of each species, PS, from species 0 to x as a function of the ligand concentrations. For

troponin C, binding to Ca^{2+}, x = 4, and there exist five species: TnC-0Ca^{2+}, TnC-1Ca^{2+}, TnC-2Ca^{2+}, TnC-3Ca^{2+}, and TnC-4Ca^{2+}. Matrix B is the output of isotopic abundances of species IS from peak 0 to peak n as a function of various Ca^{2+} binding states.

In the implementation, we normalized each row of each matrix so that their sum is equal to 1, and we required that the values in matrix B be positive. We fit the output in matrix B to the best values; this procedure requires minimizing the differences between matrix A and the product of matrix B and C. The intensity input can be the intensity of the peak centroid or its area in a peak-profile mode; the latter was used in this work so that each part in the isotopic distribution pattern was considered, in principle increasing the accuracy of the calculation. By comparing the distribution of the peaks and their area, we obtained a deuterium isotopic pattern of each peptic peptide as a function of the Ca^{2+} binding state. Changes in H-bonding or solvent accessibility for various regions of the protein induced by Ca^{2+} binding can be determined by simply analyzing the shift of the isotopic distribution.

d. Order of Ca^{2+} binding

Our hypothesis is that changes in the deuterium distributions for peptides from regions involved in Ca^{2+} binding as a function of the states of the protein (TnC-0Ca^{2+} to TnC-4Ca^{2+}) will report the order of Ca^{2+} binding. To test this hypothesis, we needed four abundant peptic peptides each representing one of the four EF hands to follow as a function of the fractional species calculation, and we were able to obtain these reporter peptides by pepsin digestion. The four peptides are doubly charged DADGGGDISVKELGTVM (28-44) containing EF-I; doubly charged, EVDEDGSGTID (63-73) containing EF-II; doubly charged FRIFDRNADG (100-109) containing EF-III; and triply charged, MKDGDKNNDGRIDF (136-149) containing EF-IV. (One set of mass spectra of these four peptic peptides from three trials are presented in **Supplemental Figure 3-6**). The outcome of the matrix-algebra calculation gave us the deuterium distributions convolved with the native distribution of C-13, N-15 and O-18 of each EF hand for the five states of Ca^{2+} binding to troponin C. We then removed all isotope components except D for these four unique peptic peptides by using the theoretical isotope ratio provided via the Isotope Simulation function in Qual Browser 2.0.7 (Xcalibur, Thermo Fisher, San Jose, CA). The isotope deconvolution process is illustrated in supplemental Figure 7. Briefly, each deuterium-containing isotopic pattern is a mixture of various numbers of deuterium-containing species (d_0, d_1, d_2...) with their isotopic species. By knowing the chemical formula for a particular peptide, we can calculate the isotope distribution (except that of D from H/DX) and remove it from the distribution, leaving a pure deuterium distribution (**Figure 5**). We submit that any slight change of the deuterium uptake can be readily revealed by this strategy.

Comparing the variation of the deuterium-distribution centroid for the four peptic peptides as a function of different Ca^{2+} bound troponin C states (Figure 5), we see that the first shift from higher to lower deuterium content (indicating onset of protection) occurs for peptic peptide 100-109 containing EF-III for the transition of TnC-0Ca^{2+} to TnC-1Ca^{2+} whereas the deuterium distributions of the peptides representing the other three EF hands remain largely unaffected. This indicates that EF-III in skeletal troponin C is first to bind Ca^{2+}, although the binding may not be complete as the D distribution continues to shift to more protection as more calcium binds. Peptic peptide 136-149 from EF-IV showed a similar but more conclusive shift from a centroid of six to four deuteriums for TnC-2Ca^{2+}, indicating that EF-IV is the second Ca^{2+} binding site. Similar to EF-III, the D distribution shows additional minor shifts as the protein continues to take up calcium. Although the shifts for EF-III and IV do not occur sharply as various states of Ca^{2+} binding are achieved, the results clearly show the higher propensity for binding Ca^{2+} by EF-III and EF-IV (~10^7 M^{-1}) than by EF-II and EF-I. Sykes and coworkers (*53*) studied the binding of Ca^{2+} to synthetic EF-III

and EF-IV peptides of troponin C by 1H-NMR. Their results show that Ca^{2+} binds to synthetic EF-III peptide; the resulting Ca^{2+}-EF-III then associates with the apo-EF-IV peptide to form a heterodimer Ca^{2+}-EF-III/EF-IV. The heterodimer then binds the second calcium to give $2Ca^{2+}$-EFIII/EFIV. Our results on the intact protein agree with this general picture of stepwise binding.

Because the N-terminal EF-I and EF-II have lower binding affinities to Ca^{2+} (~10^6 M^{-1}), they should bind after EF-III and IV. Indeed, the deuterium content (most abundant ion) of the peptic peptide containing EF-II shifts from four to two deuteriums at the transition to TnC-$3Ca^{2+}$, whereas the peptic peptide representing EF-I shifts from eight to six deuteriums at the transition to TnC-$4Ca^{2+}$. Thus, the third Ca^{2+} binds at EF-II followed by the last Ca^{2+} binding at EF-I. Sykes and coworkers (*37*) also studied Ca^{2+} binding to EF hands in N-terminus of chicken skeletal troponin C by using NMR. Although the overall binding picture for full length TnC remained unclear, they could conclude that EF-II is the first site in the N-terminus of troponin C that binds to Ca^{2+} and EF-I is the last Ca^{2+} binding site, a conclusion that is consistent with the results of H/DX presented here.

To illustrate more clearly the order of Ca^{2+} binding, we normalized the deuterium- uptake values for the four peptides to their maximum deuterium uptake. This allows us to view the relative deuterium uptake as a function of different TnC-Ca^{2+} states (**Figure 6**). The outcome clearly shows that the order of Ca^{2+} binding to the four Ca^{2+} binding sites in intact skeletal troponin C is EF-III > EF-IV > EF-II >EF-I, although there is likely to be some simultaneous binding of Ca^{2+} by EF-III and IV.

DISCUSSION

The advantage of H/DX coupled with MS is that changes in the extent of H/DX, whether caused by increased H bonding or decreased solvent accessibility or both, can be used to compare two or more states. The conclusions do not depend highly on the abundances of the various isotopomers but principally on their *m/z*. The PLIMSTEX strategy further extends the advantage of H/DX by affording, via ligand titrations at a fixed concentration of protein, the protein-ligand binding affinities. The equilibrium constants are essential for the design of an experimental approach to extract deuterium distributions for regions of a protein as a function of its binding state.

We illustrate the approach to determine the binding order of Ca^{2+} to troponin C. Although troponin C is a well-studied protein, establishing the order of Ca^{2+} binding has proven difficult. The kinetics of HDX at the protein or global level demonstrates that the protein is considerably stabilized as a consequence of Ca^{2+} binding. The differences in the apo and holo states allow the binding affinities of troponin C with Ca^{2+} to be measured in a single-titration format. The values of the equilibrium constants allow calculation of fractional species for troponin C. From H/DX experiments at known fractional species, we can extract the deuterium distribution of four regions of the protein that bind Ca^{2+}. Those distributions shift to lower mass when Ca^{2+} binds at the site, providing a basis for determining the binding order of the four Ca^{2+} ions.

Previous studies on Ca^{2+} binding to troponin C by Ca^{2+} titration (*36, 37, 52, 53, 64*) indicated the binding is cooperative and affected by pH. Those studies, however, did not give a clear outcome of the binding order of Ca^{2+} to troponin C probably because the similar binding affinities of Ca^{2+} in each terminal region of troponin C cause the states to coexist at various Ca^{2+} concentrations. Nevertheless, our results indicate the Ca^{2+} binding to skeletal troponin C occurs in the order EF-III > EF-IV > EF-II > EF-I. This determination is

attributed to the high sensitivity of MS in the H/DX platform and the ability to extract from the data specific D distributions for the five binding states of the protein.

The reasons for this trend of binding are not completely understood. Preferential binding at the C terminus is well-established. Binding details may be an outcome of the various charge states of the protein in different pH environments or the difference of the secondary and tertiary structure of the Ca^{2+} binding sites with respect to individual Ca^{2+} binding (*52*). It will be of interest to see whether this approach can be applied to determine binding orders of other proteins and ligands.

Supplementary Material

Refer to Web version on PubMed Central for supplementary material.

Acknowledgments

We thank Dr. Henry Rohrs for assistance with the LTQ-Orbitrap analysis and database searching.

Funding: This research was supported by the NCRR of the NIH (Grant No. 21 2P41RR000954) to MLG.

Abbreviations

TnC	Troponin C
PLIMSTEX	Protein Ligand Interaction by Mass Spectrometry, Titration and H/D Exchange
MS	mass spectrometry
ESI	electrospray ionization
Da	Dalton
H/DX	hydrogen/deuterium exchange
NMR	nuclear magnetic resonance
D_2O	deuterium oxide
HCl	hydrochloric acid
UPLC	ultra performance liquid chromatography
Q-TOF	quadrupole time-of-flight
MWCO	molecular weight cut off

REFERENCES

1. Filatov AGK, Bulargina TV, Gusev NB. Troponin: structure, properties, and mechanism of functioning. Biochemistry (Moscow). 1999; 64:1155–1164.
2. Grabarek Z, Tao T, Gergely J. Molecular mechanism of troponin-C function. Journal of Muscle Research and Cell Motility. 1992; 13:383–393. [PubMed: 1401036]
3. Zot AS, Potter JD. Structural aspects of troponin-tropomyosin regulation of skeletal muscle contraction. Annual Review of Biophysics and Biophysical Chemistry. 1987; 16:535–559.
4. Herzberg O, James MNG. Refined crystal structure of troponin C from turkey skeletal muscle at 2.0 A resolution. Journal of Molecular Biology. 1988; 203:761–779. [PubMed: 3210231]
5. Gulati J, Babu A, Su H, Zhang YF. Identification of the regions conferring calmodulin-like properties to troponin C. Journal of Biological Chemistry. 1993; 268:11685–11690. [PubMed: 8389360]

6. Li Y, Mui S, Brown JH, Strand J, Reshetnikova L, Tobacman LS, Cohen C. The crystal structure of the C-terminal fragment of striated-muscle - tropomyosin reveals a key troponin T recognition site. Proceedings of the National Academy of Sciences of the United States of America. 2002; 99:7378–7383. [PubMed: 12032291]
7. Kobayashi T, Solaro RJ. Calcium, thin filaments, and the integrative biology of cardia contractility. Annual Review of Physiology. 2005; 67:39–67.
8. Takeda S. Crystal structure of troponin and the molecular mechanism of muscle regulation. J Electron Microsc (Tokyo). 2005; 54:i35–41. [PubMed: 16157639]
9. Davis JP, Tikunova SB. Ca^{2+} exchange with troponin C and cardiac muscle dynamics. Cardiovasc Res. 2008; 77:619–626. [PubMed: 18079104]
10. Sun Y-B, Lou F, Irving M. Calcium- and myosin-dependent changes in troponin structure during activation of heart muscle. J Physiol. 2009; 587:155–163. [PubMed: 19015190]
11. Paul DM, Morris EP, Kensler RW, Squire JM. Structure and orientation of troponin in the thin filament. J. Biol. Chem. 2009; 284:15007–15015. [PubMed: 19321455]
12. Satyshur KA, Rao ST, Pyzalska D, Drendel W, Greaser M, Sundaralingam M. Refined structure of chicken skeletal muscle troponin C in the two- calcium state at 2.0A resolution. J. Biol. Chem. 1988; 263:1628–1647. [PubMed: 3338985]
13. Jayashree S, Terence T, George NP Jr. Conformational variation of calcium-bound troponin C. Proteins: Structure, Function, and Genetics. 1999; 37:510–511.
14. Sykes BD. Pulling the calcium trigger. Nat Struct Mol Biol. 2003; 10:588–589.
15. Vinogradova MV, Stone DB, Malanina GG, Karatzaferi C, Cooke R, Mendelson RA, Fletterick RJ. Ca^{2+}-regulated structural changes in troponin. Proceedings of the National Academy of Sciences of the United States of America. 2005; 102:5038–5043. [PubMed: 15784741]
16. Sun Y-B, Brandmeier B, Irving M. Structural changes in troponin in response to Ca^{2+} and myosin binding to thin filaments during activation of skeletal muscle. Proceedings of the National Academy of Sciences. 2006; 103:17771–17776.
17. Reece KL, Moss RL. Intramolecular interactions in the N-domain of cardiac troponin C are important determinants of calcium sensitivity of force development. Biochemistry. 2008; 47:5139–5146. [PubMed: 18410130]
18. Kawasaki H KR. Calcium-binding proteins 1: EF-hands. Protein Profile. 1994; 4:297–490.
19. Gillis TE, Marshall CR, Tibbits GF. Functional and evolutionary relationships of troponin C. Physiol. Genomics. 2007; 32:16–27. [PubMed: 17940202]
20. Calvert MJ, Ward DG, Trayer HR, Trayer IP. The importance of the carboxyl-terminal domain of cardiac troponin C in Ca^{2+}-sensitive muscle regulation. J. Biol. Chem. 2000; 275:32508–32515. [PubMed: 10921926]
21. Li M, Saude E, Wang X, Pearlstone J, Smillie L, Sykes B. Kinetic studies of calcium and cardiac troponin I peptide binding to human cardiac troponin C using NMR spectroscopy. European Biophysics Journal. 2002; 31:245–256. [PubMed: 12122471]
22. Takeda S, Yamashita A, Maeda K, Maeda Y. Structure of the core domain of human cardiac troponin in the Ca^{2+}-saturated form. Nature. 2003; 424:35–41. [PubMed: 12840750]
23. Li M, Wang X, Sykes B. Structural based insights into the role of troponin in cardiac muscle pathophysiology. Journal of Muscle Research and Cell Motility. 2004; 25:559–579. [PubMed: 15711886]
24. Li Z, Gergely J, Tao T. Proximity relationships between residue 117 of rabbit skeletal troponin-I and residues in troponin-C and actin. Biophys. J. 2001; 81:321–333. [PubMed: 11423417]
25. Li MX, Sykes BD. Role of the Structural Domain of Troponin C in Muscle Regulation: NMR Studies of Ca^{2+} binding and subsequent interactions with regions 1-40 and 96-115 of troponin I. Biochemistry. 2000; 39:2902–2911. [PubMed: 10715110]
26. Ferguson RE, Irving M, Corrie JET, Trentham DR, Sykes BD. NMR Structure of a bifunctional rhodamine labeled N-domain of troponin C complexed with the regulatory “witch” peptide from troponin I: implications for in situ fluorescence studies in muscle fibers. Biochemistry. 2003; 42:4333–4348. [PubMed: 12693929]

27. Blumenschein TMA, Stone DB, Fletterick RJ, Mendelson RA, Sykes BD. Dynamics of the C-terminal region of TnI in the troponin complex in solution. Biophys. J. 2006; 90:2436–2444. [PubMed: 16415057]
28. Wang ZY, Sarkar S, Gergely J, Tao T. Ca2(+)-dependent interactions between the C-helix of troponin-C and troponin-I. Photocross-linking and fluorescence studies using a recombinant troponin-C. J. Biol. Chem. 1990; 265:4953–4957. [PubMed: 2180953]
29. Wang Z, Gergely J, Tao T. Characterization of the Ca(2+)-triggered conformational transition in troponin C. Proceedings of the National Academy of Sciences of the United States of America. 1992; 89:11814–11817. [PubMed: 1465405]
30. Foguel D, Suarez MC, Barbosa C, Rodrigues JJ, Sorenson MM, Smillie LB, Silva JL. Mimicry of the calcium-induced conformational state of troponin C by low temperature under pressure. Proceedings of the National Academy of Sciences of the United States of America. 1996; 93:10642–10646. [PubMed: 8855232]
31. Chandra M, Dong W-J, Pan B-S, Cheung HC, Solaro RJ. Effects of protein kinase A phosphorylation on signaling between cardiac troponin I and the N-terminal domain of cardiac troponin C. Biochemistry. 1997; 36:13305–13311. [PubMed: 9341222]
32. Finley NL, Rosevear PR. Introduction of negative charge mimicking protein kinase C phosphorylation of cardiac troponin I: Effects on cardiac troponin C. J. Biol. Chem. 2004; 279:54833–54840. [PubMed: 15485824]
33. Baryshnikova OK, Li MX, Sykes BD. Defining the binding site of Levosimendan and its analogues in a regulatory cardiac troponin C-troponin I complex. Biochemistry. 2008; 47:7485–7495. [PubMed: 18570382]
34. Li MX, Robertson IM, Sykes BD. Interaction of cardiac troponin with cardiotonic drugs: A structural perspective. Biochemical and Biophysical Research Communications. 2008; 369:88–99. [PubMed: 18162171]
35. Spyracopoulos L, Sykes BD. Structure, Dynamics, and Thermodynamics of the Structural Domain of Troponin C in Complex with the Regulatory Peptide 1-40 of Troponin I. Biochemistry. 2001; 40:10063–10077. [PubMed: 11513585]
36. Olle T, Torbjorn D, Sture F, Eva T. Calcium and Cadmium Binding to Troponin C. European Journal of Biochemistry. 1983; 134:453–457. [PubMed: 6309513]
37. Li MX, Gagne SM, Tsuda S, Kay CM, Smillie LB, Sykes BD. Calcium binding to the regulatory N-domain of skeletal muscle troponin C occurs in a stepwise manner. Biochemistry. 1995; 34:8330–8340. [PubMed: 7599125]
38. Yamada K. Thermodynamic analyses of calcium binding to troponin C, calmodulin and parvalbumins by using microcalorimetry. Molecular and Cellular Biochemistry. 1999; 190:39–45. [PubMed: 10098967]
39. Bobst CE, Abzalimov RR, Houde D, Kloczewiak M, Mhatre R, Berkowitz SA, Kaltashov IA. Detection and characterization of altered conformations of protein pharmaceuticals using complementary mass spectrometry-based approaches. Analytical Chemistry. 2008; 80:7473–7481. [PubMed: 18729476]
40. Englander S. Hydrogen exchange and mass spectrometry: A historical perspective. Journal of The American Society for Mass Spectrometry. 2006; 17:1481–1489. [PubMed: 16876429]
41. Konermann L, Pan J, Liu Y-H. Hydrogen exchange mass spectrometry for studying protein structure and dynamics. Chemical Society Reviews. 2011; 40:1224–1234. [PubMed: 21173980]
42. Bou-Assaf GM, Chamoun JE, Emmett MR, Fajer PG, Marshall AG. Advantages of isotopic depletion of proteins for hydrogen/deuterium exchange experiments monitored by mass spectrometry. Analytical Chemistry. 2010; 82:3293–3299. [PubMed: 20337424]
43. Chalmers MJ, Busby SA, Pascal BD, West GM, Griffin PR. Differential hydrogen/deuterium exchange mass spectrometry analysis of protein-ligand interactions. Expert Review of Proteomics. 2011; 8:43–59. [PubMed: 21329427]
44. Engen JR. Analysis of protein conformation and dynamics by hydrogen/deuterium exchange MS. Analytical Chemistry. 2009; 81:7870–7875. [PubMed: 19788312]

45. Sperry JB, Shi X, Rempel DL, Nishimura Y, Akashi S, Gross ML. A Mass Spectrometric Approach to the Study of DNA-Binding Proteins: Interaction of Human TRF2 with Telomeric DNA. Biochemistry. 2008; 47:1797–1807. [PubMed: 18197706]
46. Hopper ED, Roulhac PL, Campa MJ, Patz Jr EF, Fitzgerald MC. Throughput and Efficiency of a Mass Spectrometry-Based Screening Assay for Protein-Ligand Binding Detection. Journal of the American Society for Mass Spectrometry. 2008; 19:1303–1311. [PubMed: 18653356]
47. Kowlessur D, Tobacman LS. Troponin Regulatory Function and Dynamics Revealed by H/D Exchange-Mass Spectrometry. Journal of Biological Chemistry. 2010; 285:2686–2694. [PubMed: 19920153]
48. Bou-Assaf GM, Chamoun JE, Emmett MR, Fajer PG, Marshall AG. Complexation and calcium-induced conformational changes in the cardiac troponin complex monitored by hydrogen/deuterium exchange and FT-ICR mass spectrometry. International Journal of Mass Spectrometry In Press, Corrected Proof.
49. Zhu MM, Rempel DL, Du Z, Gross ML. Quantification of Protein-Ligand Interactions by Mass Spectrometry, Titration, and H/D Exchange: PLIMSTEX. Journal of the American Chemical Society. 2003; 125:5252–5253. [PubMed: 12720418]
50. Zhu MM, Chitta R, Gross ML. PLIMSTEX: a novel mass spectrometric method for the quantification of protein-ligand interactions in solution. International Journal of Mass Spectrometry. 2005; 240:213–220.
51. Zhu MM, Rempel DL, Gross ML. Modeling data from titration, amide H/D exchange, and mass spectrometry to obtain protein-ligand binding constants. Journal of the American Society for Mass Spectrometry. 2004; 15:388–397. [PubMed: 14998541]
52. Iida S. Calcium Binding to Troponin C. II. A Ca2+ Ion Titration Study with a Ca2+ Ion Sensitive Electrode. J Biochem. 1988; 103:482–486. [PubMed: 3392001]
53. Gary SS, Robert SH, Brian DS. Stoichiometry of calcium binding to a synthetic heterodimeric troponin-C domain. Biopolymers. 1992; 32:391–397. [PubMed: 1623134]
54. Bai Y, Milne JS, Mayne L, Englander SW. Primary structure effects on peptide group hydrogen exchange. PROTEINS: Structure, Function, and Genetics. 1993; 17:75–86.
55. Houdusse A, Love ML, Dominguez R, Grabarek Z, Cohen C. Structures of four Ca2+-bound troponin C at 2.0 A resolution: further insights into the Ca2+-switch in the calmodulin superfamily. Structure. 1997; 5:1695–1711. [PubMed: 9438870]
56. Shaw GS, Golden LF, Hodges RS, Sykes BD. Interactions between paired calcium-binding sites in proteins: NMR determination of the stoichiometry of calcium binding to a synthetic troponin-C peptide. Journal of the American Chemical Society. 1991; 113:5557–5563.
57. Khamir M, Adam DH, Raghunandan K, Peter JW, Jennifer JL. A computational approach to inferring cellular protein-binding affinities from quantitative fluorescence resonance energy transfer imaging. PROTEOMICS. 2009; 9:5371–5383. [PubMed: 19834887]
58. Lee F, Samantha R, Dan F. Determination of protein-ligand binding affinity by NMR: observations from serum albumin model systems. Magnetic Resonance in Chemistry. 2005; 43:463–470. [PubMed: 15816062]
59. Mayhood TW, Windsor WT. Ligand binding affinity determined by temperature-dependent circular dichroism: Cyclin-dependent kinase 2 inhibitors. Analytical Biochemistry. 2005; 345:187–197. [PubMed: 16140252]
60. Bains G, Freire E. Calorimetric determination of cooperative interactions in high affinity binding processes. Analytical Biochemistry. 1991; 192:203–206. [PubMed: 2048721]
61. Monfregola L, Vitale RM, Amodeo P, Luca SD. A SPR strategy for high-throughput ligand screenings based on synthetic peptides mimicking a selected subdomain of the target protein: A proof of concept on HER2 receptor. Bioorganic & Medicinal Chemistry. 2009; 17:7015–7020. [PubMed: 19733086]
62. Blow N. Proteins and proteomics: life on the surface. Nat Meth. 2009; 6:389–393.
63. Rempel DL, Zhao J, Giblin DE, Gross ML. Probing Ca2+-Induced Conformational Changes in Porcine Calmodulin by H/D Exchange and ESI-MS: Effect of Cations and Ionic Strength. Biochemistry. 2003; 42:15388–15397. [PubMed: 14690449]

64. Potter JD, Gergely J. The calcium and magnesium binding sites on troponin and their role in the regulation of myofibrillar adenosine triphosphatase. J. Biol. Chem. 1975; 250:4628–4633. [PubMed: 124731]

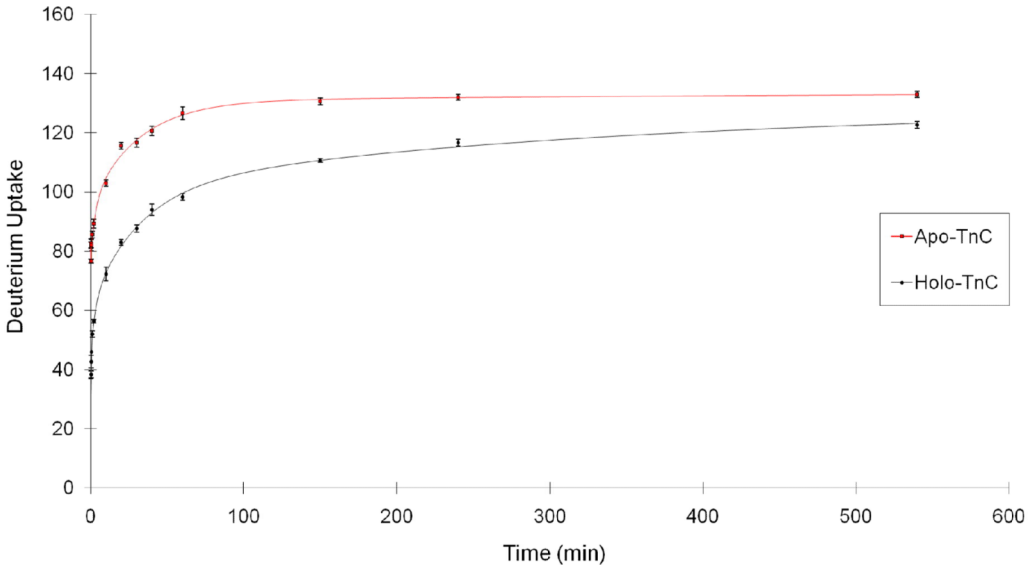

Figure 1.

Kinetics of H/D exchange for rabbit skeletal troponin C. Apo-troponin C in 3 mM EGTA (squares, red) shows more extensive D uptake than holo troponin C in 1 mM $CaCl_2$ (diamonds, black). The fitted curves are shown as solid lines.

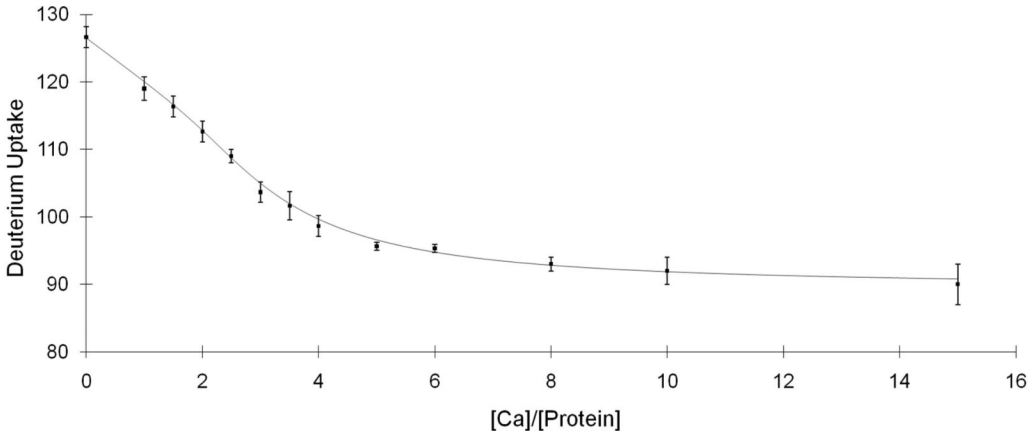

Figure 2.
PLIMSTEX curve of Troponin C titrated with Ca^{2+} and followed by MS-based H/DX. The concentration of the protein for the titration was 0.3 μM.

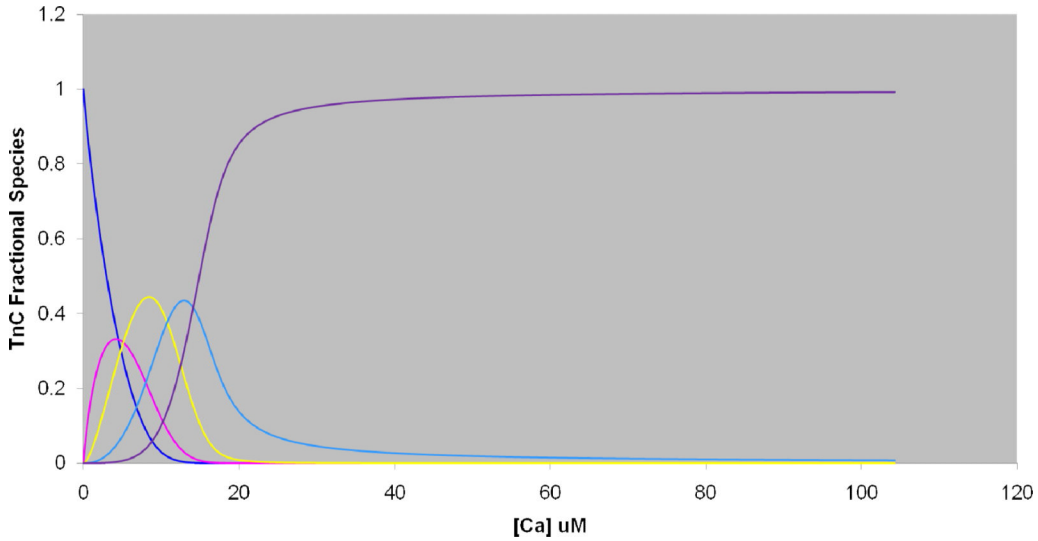

Figure 3.

Fractional species curves showing the distribution of each TnC:xCa^{2+} as a function of Ca^{2+} concentration (μM). (Blue: zero Ca^{2+}-bound; Pink: 1 Ca^{2+}-bound;, Yellow: 2 Ca^{2+}-bound; Light blue: 3 Ca^{2+}-bound; Purple: 4 Ca^{2+}- bound).

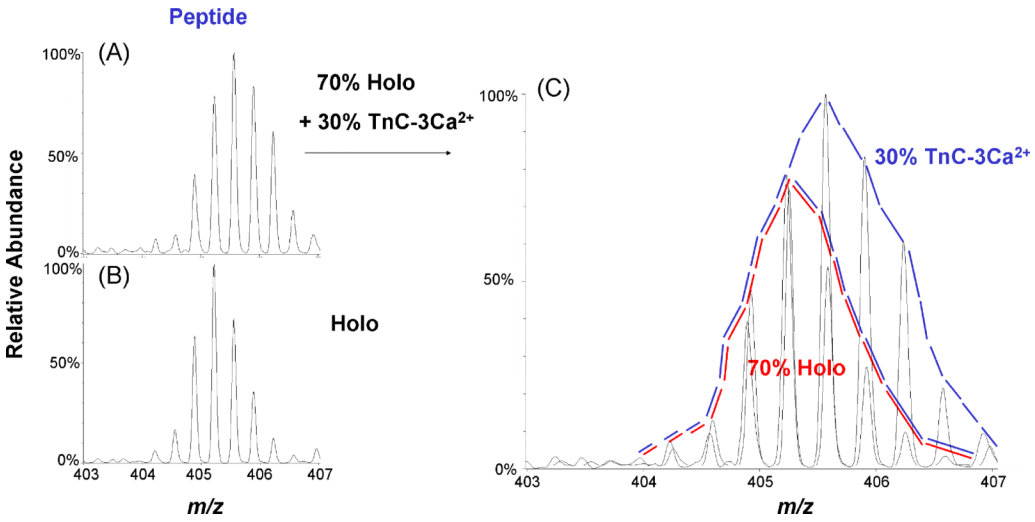

Figure 4.

(A) Deuterium-containing isotopic distribution of the triply charged peptic peptide 100-109 (FRIFDRNADG). The distribution can be represented as a mixture of 70% holo (TnC-4Ca^{2+}, red area in C) and 30% TnC-3Ca^{2+} states as shown in (C), which is an enlarged view of A. (B) Deuterium-containing isotopic distribution of triply charged peptic peptide 100-109 (FRIFDRNADG). The distribution represents 100% Holo state (TnC-4Ca^{2+}) in 1 mM $CaCl_2$. (C) Enlarged view of (A).

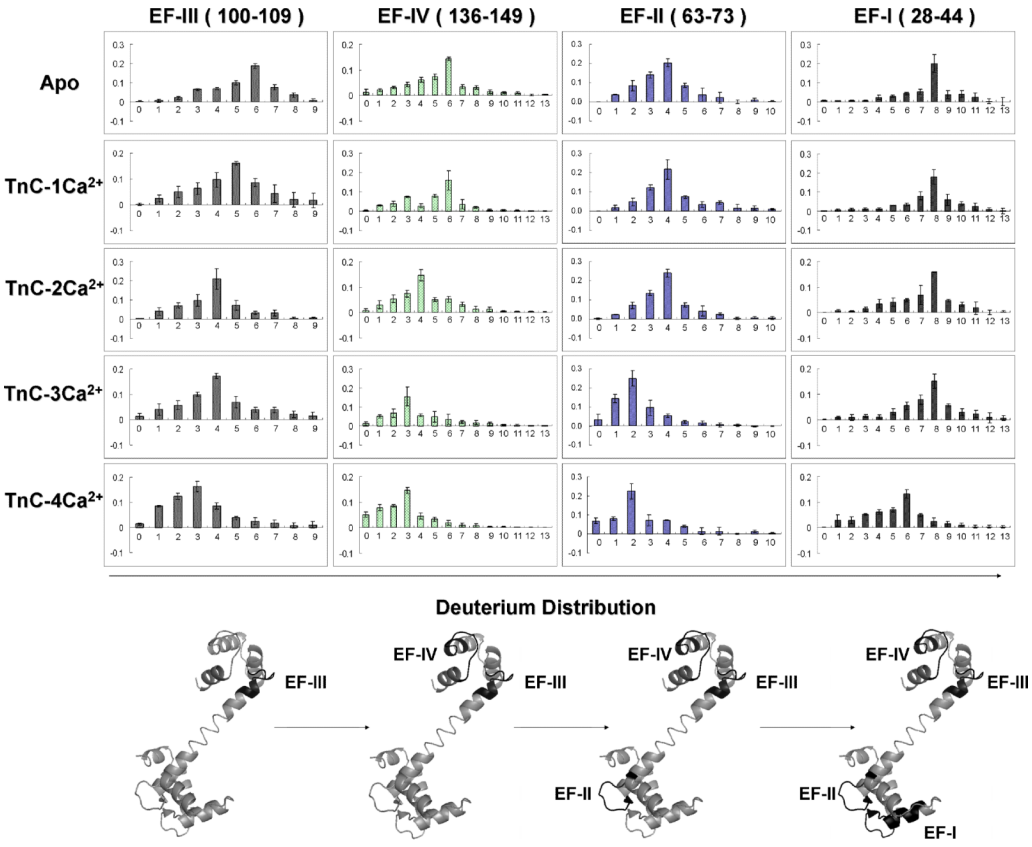

Figure 5.

Top: Each column represents the deuterium distributions of the peptic peptide of EF hands: III, IV, II, I (left to right). Each row represents the various Ca^{2+} bound TnC states: Apo (Absent Ca^{2+}) to 4 Ca^{2+} bound TnC (top to bottom). Bottom: X-ray crystal structure of rabbit skeletal troponin C (PDB: 1TCF) in gray, and the four EF hands are in black.

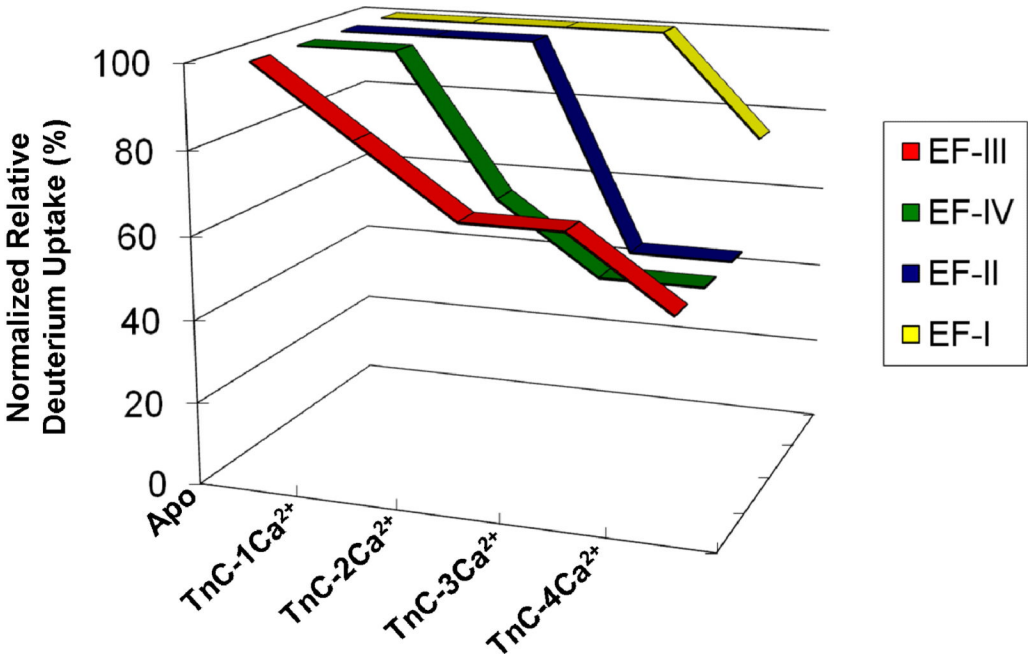

Figure 6.

A plot of the normalized relative deuterium uptake based on the centroids of the deuterium distributions for four peptic peptides containing the four EF hands as a function of various Ca^{2+}-bound TnC states.

Table 1

Numbers of amide hydrogen undergoing exchange for D for apo and holo troponin C. The kinetic modeling used four fixed exchange rate constants and “binned” the number of amides with respect to the rate constants.

Kinetic Fit	# of H's per fixed-rate bin			
k (min^{-1})	10	1	0.1	0.01
Apo	79 ± 1	1 ± 1	16 ± 3	37 ± 4
Holo	26 ± 2	24 ± 2	3 ± 2	61 ± 3

Table 2

Four Ca^{2+} binding constants of troponin C obtained by fitting PLIMSTEX titration curves.

K	Experimental Value	Literature Values
K_1	$(5.3 \pm 4.7) \times 10^7$ M^{-1}	2×10^7 M^{-1} (1);$(2.1 \pm 0.7) \times 10^7$ M^{-1}(64)
K_2	$(1.8 \pm 0.8) \times 10^7$ M^{-1}	2×10^7 M^{-1} (1);$(2.1 \pm 0.7) \times 10^7$ M^{-1}(64)
K_3	$(4.2 \pm 0.9) \times 10^6$ M^{-1}	5×10^6 M^{-1} (20);$(3.2 \pm 1.3) \times 10^5$ M^{-1}(64)
K_4	$(1.6 \pm 0.6) \times 10^6$ M^{-1}	5×10^6 M^{-1} (20) ;$(3.2 \pm 1.3) \times 10^5$ M^{-1}(64);
D_4	38 ± 1	N/A
D_0	127 ± 1	N/A
RMS	0.62	

Table 3

Various solution concentrations chosen for H/DX to determine the order of binding of Ca^{2+} with troponin C. The values are calculated fractional species of each Ca^{2+}-bound TnC species and are taken from the fractional species curves in Figure 3.

[Ca] μM	TnC-0Ca	TnC-1Ca	TnC-2Ca	TnC-3Ca	TnC-4Ca
0	100.0%	0.0%	0.0%	0.0%	0.0%
8.4	7.4%	19.7%	44.5%	23.7%	4.7%
10.4	2.3%	10.4%	39.8%	35.6%	11.9%
12.1	0.0%	4.9%	29.7%	42.6%	22.8%
13.8	0.0%	0.0%	18.2%	43.1%	38.7%
16.7	0.0%	0.0%	0.0%	29.1%	70.9%
2000	0.0%	0.0%	0.0%	0.0%	100.0%